Pergamon

Cement and Concrete Research 30 (2000) 907–914

CEMENT AND CONCRETE RESEARCH

Characteristics of high-performance steel fiber-reinforced concrete subject to high velocity impact

Xin Luo[a,*], Wei Sun[a], Sammy Y.N. Chan[b]

[a]*Department of Materials Science and Engineering, Southeast University, Nanjing 210096, People's Republic of China*
[b]*Wong & Cheng Consulting Engineers Ltd., Hong Kong, People's Republic of China*

Received 22 July 1999; accepted 6 March 2000

Abstract

Targets made of high-performance steel fiber-reinforced concrete (HPSFRC), which was produced by fluidized mortar, steel fibers and casting process of mortar infiltrating and vibrating, were subject to high velocity impact of projectile and compared with those targets made of reinforced high strength concrete (RHSC). Test results show when impacted by projectiles at high speed, the RHSC targets exhibited smash failure, while HPSFRC targets remained intact with several radial cracks in the front faces penetrated by projectiles and some minor cracks in the side faces. The projectiles were either embedded in or rebounded from HPSFRC targets. Relationship between the resistance of the targets against impact and the parameters concerned was analyzed. Based on the dimensional analysis, it is possible to predict the penetration performance in a real situation by using the test results from a simulation test. Besides, the relationship between penetration depth in CZ targets and the dimensionless speed of projectile was built by regressing the test results. © 2000 Elsevier Science Ltd. All rights reserved.

Keywords: High performance; Steel fiber; Impact; Dimensional analysis

1. Introduction

Development of modern civil engineering includes an urgent need to develop higher performance engineering materials possessing high strength, toughness, energy absorption, durability, etc. High-performance steel fiber-reinforced concrete (HPSFRC), which made remarkable advances during recent years [1,2], is an important high performance concrete (HPC), especially in some repair work in highway pavement, bridge deck, roof, etc. [3,4]. However, very little research work on HPSFRC behaviors when suffering high velocity impact has been carried out so far due mainly to its complexity and lack of effective methods. It is much more difficult to quantitatively investigate dynamic properties of material than to qualitatively study static or quasi-static properties. This paper carried out an experimental and simulative investigation on two series of HPSFRC compared with reinforced high strength concrete (RHSC) when they were subject to high velocity impact. It provides valuable information on the characteristics of HPSFRC resisting impact.

2. Materials, mix proportions, and test method

2.1. Materials, mix proportions for targets

Materials used in the experimental program are as follows:

Cement: type I Portland cement conforming to ASTM C150-89.
Fly ash: fly ash meeting the requirement of ASTM C618.
Admixtures: water reducer (Xp-II and TMS), BC-I retarder.
Fine aggregate: river sand with fineness modulus of 2.6.
Coarse aggregate: crushed limestone, continuous grading with maximum size of 20 mm.
Fibers: two types of steel fibers (CZ, YL) with different geometry were chosen, as shown in Table 1.

* Corresponding author. Tel.: +86-25-379-4619; fax: +86-25-771-2719.
E-mail address: luoxin@seu.edu.cn (X. Luo).

PII: S0008-8846(00)00255-6

Table 1
The steel fibers used in the experiment

Type of steel fiber	Shape of the fiber	Length of the fiber (mm)	Fiber aspect ratio
CZ	—	31	60
YL	–	21	35

The high velocity impact tests were conducted on two series of targets. One series was the target made of HPSFRC and the other target made of RHSC. HPSFRC targets included two types: YL targets containing YL steel fiber and CZ targets containing CZ steel fiber. Detailed information on mix proportions for the targets is presented in Table 2.

The HPSFRC targets were produced by fluidized mortar, steel fibers, and the manufacturing process combined mortar infiltration and vibration [5]. Steel fibers were preplaced in a mould to a certain volume fraction of its full capacity forming fiber network. Then the fiber network was infiltrated by read-made fluidized mortar and vibrated. Same steps were repeated until an analogue target was completely cast. Shape, size of the analogue targets and the reinforcing bars arranged in RHSC targets were as given in Fig. 1.

2.2. Test method

All the targets were conducted impact test after 28-day curing in a condition (20 ± 5°C, R.H. > 60%). The projectile used in the impact test was armor penetration projectile of diameter 37 mm and weight about 0.9 kg. Shape and size of the projectile are shown in Fig. 2. Speed of the projectile at the moment when impact happened was measured and recorded by a photoelectric device. A target penetrated by a projectile is shown in Fig. 2 as well. The target was confined in a rigid steel shelf and its front face was normally to the direction in which the projectile impacted.

3. Test results and discussion

3.1. Experimental observations

The RHSC targets were broken thoroughly into several parts even though impacted by slower velocity projectiles so that no test information (such as the deflection degree, penetration depth of the projectiles) could be obtained. RHSC targets were smash destroyed (as shown in Fig. 3(b)). However, under higher velocity projectile impact (speed between 364.9 and 378.3 m/s) HPSFRC targets remained intact, with radial cracks on the front faces. Projectiles were embedded in all the YL targets and rebounded from all the CZ targets (shown in Fig. 3(c) and (d)).

For composite targets, the most important characterizing the response of the structure is the variety and complexity of the damage and subsequent failure mode. The response generated is interactions occurring between the projectile and material structure. In other words, the response of the composites is affected by the composite constitutive equations, failure of constituent materials, the interface bond between fiber and material, the stress wave effects, and so on. Two principal effects, associated with the response to impact, can be identified as inertial effect of impacting bodies and the associated wave propagation phenomenon [6]. Stress wave containing considerable energy was produced in the targets when the targets were impact by the projectiles at high speed. The stress wave was reflected at interfaces and surfaces in the targets and interacted to produce tensile stress [7]. For high strength concrete, the tensile strength is far more less than the compressive strength. Cracks are more prone to initiate and propagate in RHSC targets due to the brittleness of the material. Thus, RHSC target collapse in a smash manner. Addition of fibers in brittle material can significantly restraining the initiation and propagation of cracking by the bridging effect and subsequently change the failure mode from a brittle manner to a pseudo-plastic

Table 2
Mix proportions and mechanical properties of the concrete for the targets

Items	HPSFRC target	RHSC target
Cement (kg/m^3)	1062.0	328.0
Water (kg/m^3)	276.1	85.3
Fine aggregates (kg/m^3)	1062.0	446.1
Coarse aggregates (kg/m^3)	–	1600.6
Admixture (kg/m^3)	Xp-II water reducer: 15.9, BC-I retarder: 2.7	TMS water reducer: 13.1
Steel fibers	CZ: V_f = 7%, YL:V_f = 10%	–
Reinforcing bars[a]	–	6 mm @ 150 mm
Compressive strength at 28 days (MPa)[b]	116.1 (for CZ), 107.1 (for YL)	72.4[c]
Flexural strength at 28 days (MPa)[b]	54.6 (for CZ), 36.5 (for YL)	–

[a] With a reinforcing bar of 6 mm diameter and arranged with space of 150 mm.

[b] Compressive and flexural strength was the test results of cubic (100 × 100 × 100 mm^3) and beam (100 × 100 × 400 mm^3) specimens after 28-day curing (20 ± 5°C, R.H. 95%).

[c] The compressive strength without reinforcing bars.

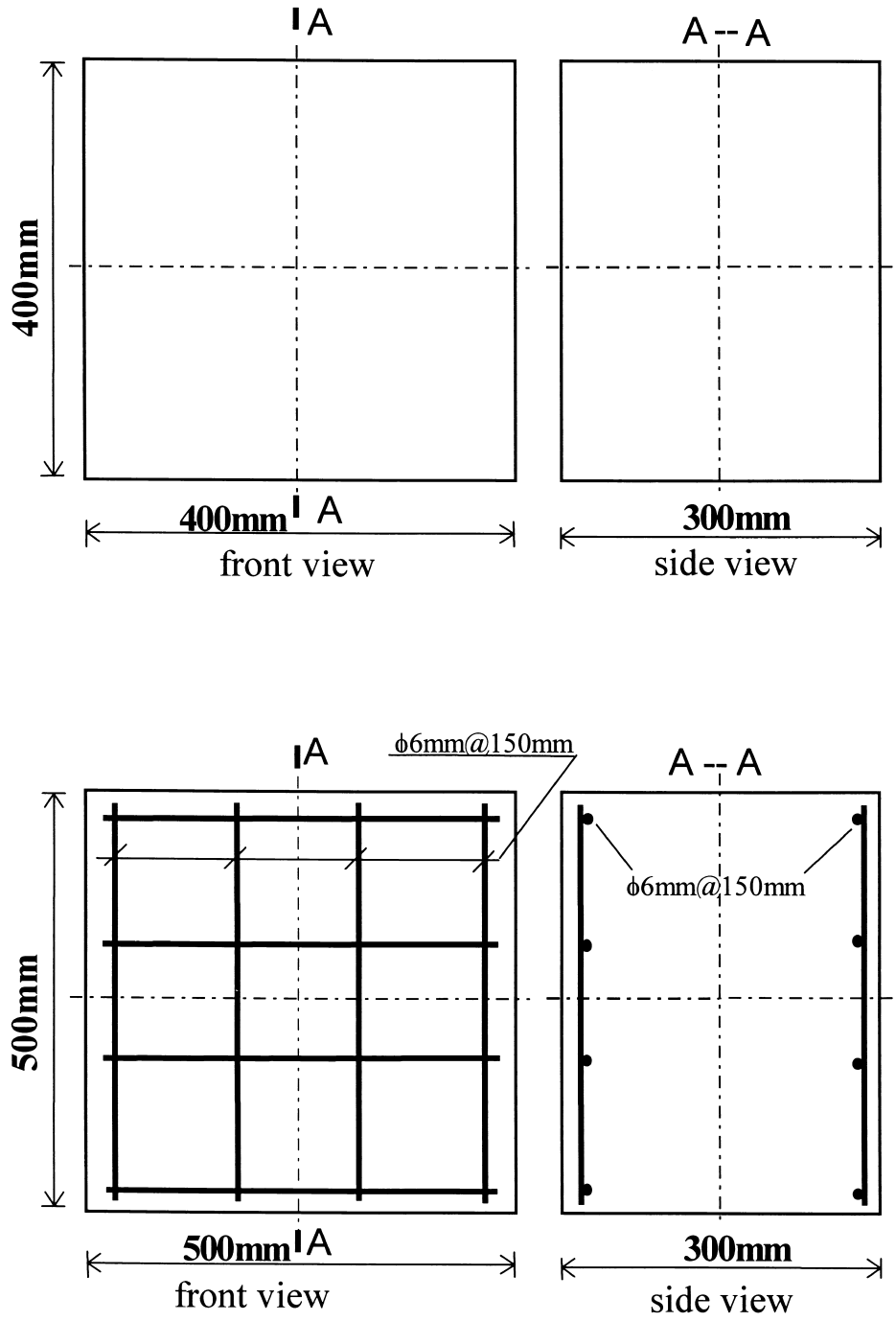

Fig. 1. HPSFRC and RHSC targets. (a) HPSFRC target. (b) RHSC target.

manner. From the test results, the back faces of all the HPSFRC targets remained uncracked and there were only some minor cracks in the side faces. Multiple layers of steel fibers in a HPSFRC target were formed during casting when the fibers were placed in batches in a mould. Although precautions were taken for casting process, there was inevitable weakness between the layers. Thus, cracks were more easily initiated at the weakness. The cracks in the side faces of YL targets were wider than those in CZ targets, because the YL steel fiber were relatively short and with smaller aspect ratio so that YL fiber generally had more tendency of two-dimensional distribution than CZ steel fiber. Therefore, both the producing process and fiber geometrical characteristics had significant effect on the behavior of HPSFRC to resist impact.

3.2. Solution based on the dimensional analysis

In order to evaluate the response of system subject to impact loading, it is important to classify the type and

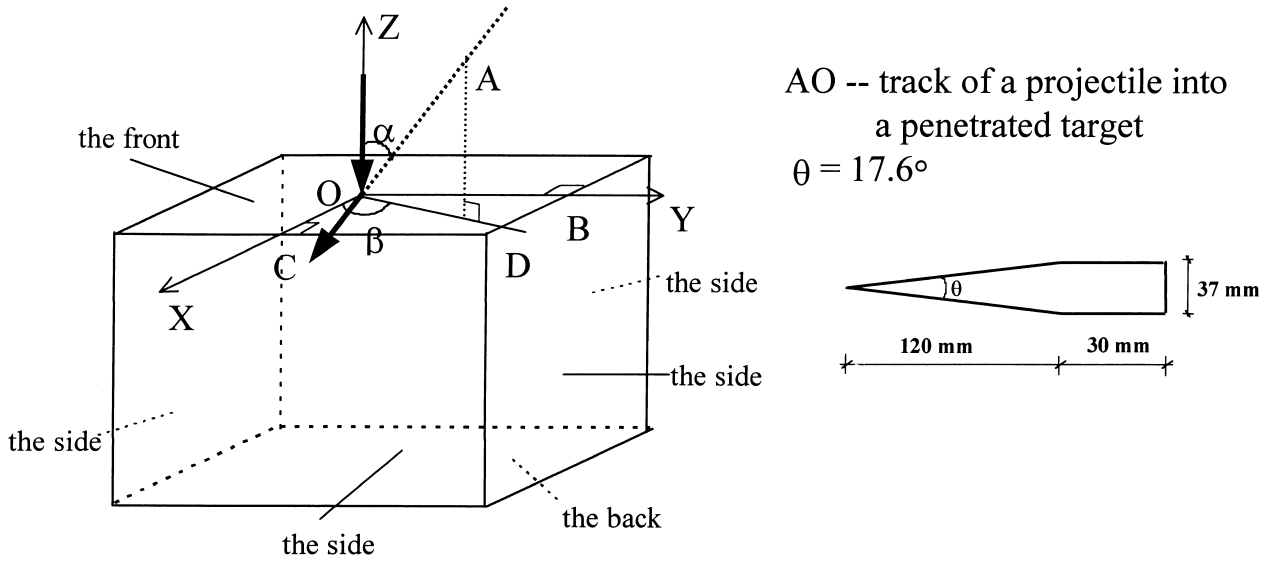

Fig. 2. A target impacted by a projectile. (a) A target. (b) A projectile.

regimes of loading, projectile/target interaction, and so on. In this test, the detailed information is given in Table 3.

Behaviors of target subject to impact are very complicated, depending on material factors (such as matrix properties, fiber characteristic) as well as test condition factors (such as the mass, speed of projectiles). Due to the complicated response of target subject to high velocity impact and high cost of undertaking the full-scale impact test in a true situation, a simulation test based on dimensional analysis, which is especially suitable for investigating dynamic properties of material [8,9], is of practical significance.

Dimensional analysis is a method to establish relationship between different quantities or variables on basis of dimensional homogeneity. There are two kinds of dimensions, i.e., the fundamental dimension and the derived dimension. Fundamental dimensions are independent in the sense that it is not possible to express it as a combination of the others, while derived dimension can be represented as power and multiplier of the fundamental dimensions. For example, length (L), time (T), and mass (M) are fundamental dimensions; velocity (V) is a derived dimension and has its dimensional representation as $V = L^1T^{-1}M^0 = LT^{-1}$.

In dimensional analysis, the π theorem (pi theorem) is of the most practical importance. π theorem can be briefly expressed as follows. In a physics equation with n variables

$$f(x_1, x_2, \ldots, x_n) = 0 \tag{1}$$

where x_1, x_2, ... , x_n are n variables.

If m of the n variables are the independent ones, then Eq. (1) always can be rewritten in the form as Eq. (2)

$$F(\pi_1, \pi_2, \ldots, \pi_{n-m}) = 0 \tag{2}$$

where π_1, π_2, ... , π_{n-m} are $n-m$ dimensionless variables defined in terms of the m independent variables.

For the targets subject to high velocity impact by projectiles, the capability of resisting the penetration is of interest. The penetration depth of projectile into the targets could be basically expressed as a function with regard to the following factors concerned

$$L_t = f(\rho_p, \rho_t, E_p, E_t, \nu_p, \nu_t, Y_p, Y_t, L_p, u_p, \varphi) \tag{3}$$

in which L_t is the the penetration depth of projectile into target, ρ_p and ρ_t are the density of projectile and target, respectively, E_p and E_t are the modulus of elasticity of projectile and target, respectively, ν_p and ν_t are the Poisson's ratio of projectile and target, respectively, Y_p and Y_t are the yield strength of projectile and target, respectively, L_p, u_p, and φ are the feature size, impact speed and angle of projectile, respectively.

There are 11 variables in Eq. (3), in which dimensions of three qualities are $\rho = L^{-3}T^0M^1$, $Y = L^{-1}T^{-2}M^1$, and $L = L^1T^0M^0$. The relative exponent determinant is

$$\begin{vmatrix} -3 & 0 & 1 \\ -1 & -2 & 1 \\ 1 & 0 & 0 \end{vmatrix} = 2 \neq 0.$$

Thus, ρ, Y and L are independent with each other. Eq. (3) can be expressed by using eight dimensionless variables in terms of the three qualities, i.e.,

$$\frac{L_t}{L_p} = g\left(\frac{\rho_p}{\rho_t}, \frac{E_p}{Y_t}, \frac{E_t}{Y_t}, \nu_p, \nu_t, \frac{Y_p}{Y_t}, \frac{u_p}{\sqrt{Y_t/\rho_t}}, \varphi\right). \tag{4}$$

If the materials of both projectile and target are kept unchanged in simulation test and in true condition, then six dimensional variables related to material are constant, therefore, Eq. (4) can be written as Eq. (5)

$$\frac{L_t}{L_p} = g\left(\frac{u_p}{\sqrt{Y_t/\rho_t}}, \varphi\right). \quad (5)$$

Furthermore, assuming u_p and φ in the simulation test and true situation are the same, then $u_p/\sqrt{Y_t/\rho_t}$ and φ are constant too. Thus, Eq. (6)

$$\left(\frac{L_t}{L_p}\right)_m = \left(\frac{L_t}{L_p}\right)_r \quad (6)$$

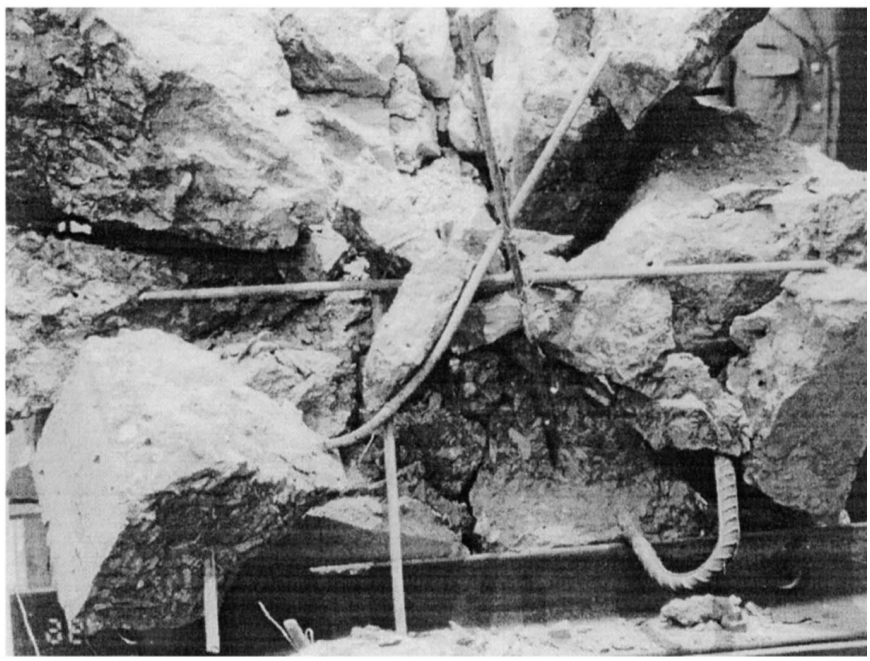

Fig. 3. The targets before and after impact test. (a) Targets before impact test. (b) RHSC target after impact test. (c) HPSFRC target (CZ) after impact with projectile rebounded. (d) HPSFRC target (YL) after impact with projectile imbedded.

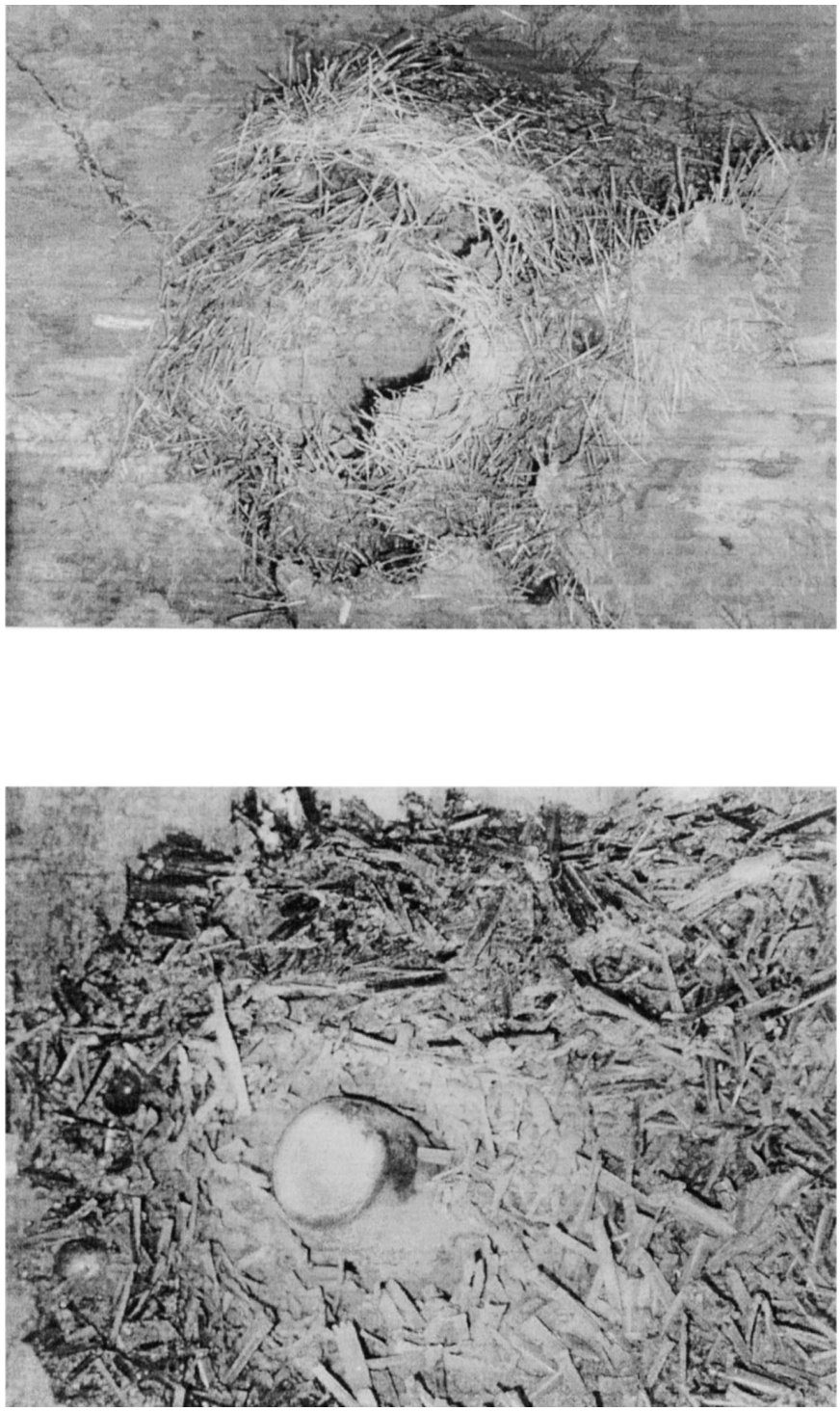

Fig. 3 (*continued*).

in which subscripts m and r represent in simulation test and in a real situation, respectively.

It is denoted that impact effect between simulation test and real situation is geometrically similar. If the proportion scale in the simulation test is $1/\alpha$, then the $(L_t)_r$ can be derived by using the test result $(L_t)_m$, that is Eq. (7)

$$(L_t)_r = \alpha(L_t)_m. \tag{7}$$

Based on the above analysis, taking into consideration the primary factors influencing the penetration of projectile into

Table 3
Test results of impact on the targets

Samples[a]	Mass of projectile (g)	Speed of projectile (m/s)	Location of impact (cm)	Angle of penetration	Penetration depth (cm)[b]	Final status of projectile
CZ-1	901.0	368.1	OC = 15.0, OB = 19.5	$\alpha = 30°$ $\beta = 114°$	13.2	rebounded 5 m
CZ-2	901.5	374.8	OC = 18.0, OB = 15.5	$\alpha = 30°$, $\beta = 32°$	14.7	rebounded
CZ-3	905.6	369.1	OC = 16.2, OB = 19.0	$\alpha = 23°$, $\beta = 35°$	13.2	rebounded 12 m
CZ-4	904.2	378.3	OC = 17.2, OB = 16.5	$\alpha = 19°$, $\beta = 42°$	15.1	rebounded 15 m
CZ-5	909.0	374.9	OC = 17.5, OB = 14.5	$\alpha = 18°$, $\beta = 30°$	15.0	rebounded 3 m
YL-1	904.2	368.7	OC = 18.0, OB = 20.2	$\alpha = 18°$, $\beta = 212°$	16.1	imbedded
YL-2	906.0	364.9	OC = 12.5, OB = 20.8	$\alpha = 28°$, $\beta = 126°$	17.7	imbedded
RHSC-1	909.5	301.5	–	–	–	–
RHSC-2	909.5	326.5	–	–	–	–
RHSC-3	909.5	300.4	–	–	–	–
RHSC-4	903.0	334.3	–	–	–	–
RHSC-5	902.5	321.7	–	–	–	–

[a] Samples CZ-1–CZ-5, YL-1, and YL-2 are the HPSFRC samples.
[b] Penetration depth in the direction perpendicular to the penetrated surface.

target, relationship between three dimensionless parameters could be given as

$$\frac{p}{D_p} = k\left(\frac{\rho_p}{\rho_t}\right)^a \left(\frac{u_p}{\sqrt{Y_t/\rho_t}}\right)^b \tag{8}$$

where p is the depth of projectile penetration in a target, D_p is the diameter of a projectile, and k, a, and b are the coefficients.

In this experimental investigation, Eq. (8), with regard to the CZ targets subject to high velocity impact was obtained as given in Eq. (9) and Fig. 4 by regressing the results of simulation test.

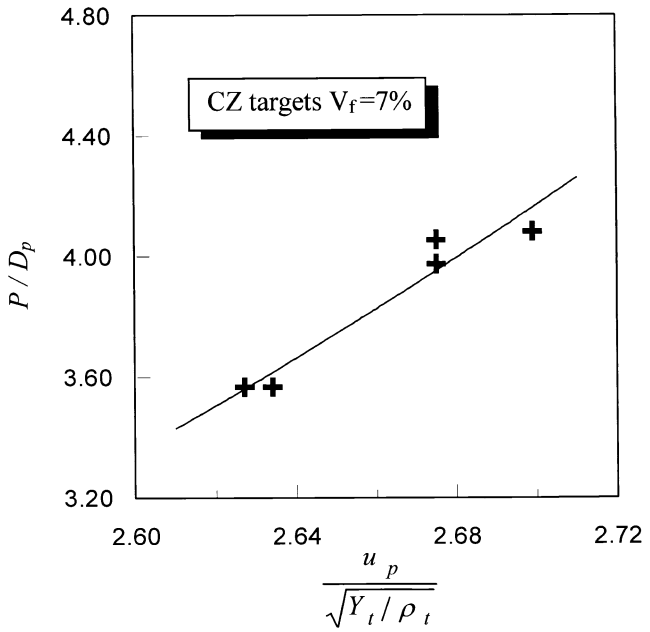

Fig. 4. Relationship between dimensionless speed of projectiles and the penetration depth in CZ targets.

$$\frac{p}{D_p} = 0.002421\left(\frac{u_p}{\sqrt{Y_t/\rho_t}}\right)^{5.6928} \tag{9}$$

In Eq. (9) and Fig. 4, the experimental data from the simulation test are preliminary and narrow to a certain degree. More test data with wider extension are being undertaken in a further investigation.

4. Conclusions

From the test results and the above discussion, the behaviors of HPSFRC to resist impact was much better than that of RHSC. Test observations show when impacted by projectiles at high speed, the RHSC targets exhibited smash failure while all the HPSFRC targets remain intact with several radial cracks on the front faces and some minor cracks on the side faces. The projectiles were either imbedded in or rebounded from HPSFRC targets. Relationship between the resistance against impact and the concerned parameters of the targets was analyzed. Based on the dimensional analysis, it is possible to predict the penetration performance in true situation by using the test results in a simulation test. Besides, the relationship between penetration depth in CZ targets and the dimensionless speed of projectile was built by regressing the test results, although the data were narrow to some degree.

Acknowledgments

This research was a part of a key project supported by National Nature Science Foundation Grant No. 59938170. The authors also wish to thank Mr. C.Q. Qi and Mr. H.S. Chen for their kind assistance in the experimental work.

References

[1] H.W. Reinhardt, A.E. Naaman, High Performance Fiber Reinforced Cement Composites, E & FN Spon, London, 1992.
[2] A.E. Naaman, H.W. Reinhardt, Proceedings of the HPFRCC2, E & FN Spon, London, 1996.
[3] A.E. Naaman, J.K. Wight, H. Abdou, SIFCON connections for seismic resistant frames, Concr Int 9 (11) (1987) 34–39.
[4] R. Breitenbücher, High performance fibre concrete SIFCON for repairing environmental structures, in: H.W. Reinhardt, A.E. Naaman (Eds.), Proceedings of the HPFRCC3, RILEM Publications, Cachan, France, 1999, pp. 585–594.
[5] X. Luo, A study on preparation, mechanical properties, anti-penetration behavior, and relative mechanisms of HPSFRCC, Master Thesis, Southeast University, 1997.
[6] R.L. Sierakowski, Dynamic Loading and Characterization of Fiber-Reinforced Composites, Wiley, New York, 1997.
[7] T.Y. Fan, An Introduction of Fracture Dynamic Mechanics, Beijing Institute of Technology Press, Beijing, 1990.
[8] G.C. Sun, Simulation Test of Armor Penetration, Technical Report of the Mechanics Research Institute of Chinese Academy of Science.
[9] D.S. Wen, Fluid Mechanics Engineering, Higher Education Press, Beijing, 1990.